Dynamics, Alterations, and Consequences of Minimally Invasive Intraocular Pressure Elevation in Rats

Oliver W. Gramlich,[1] Theresa C. S. Lueckner,[1] Maren Kriechbaum,[1] Julia Teister,[1] Xue Tao,[1] Harald D. von Pein,[2] Norbert Pfeiffer,[1] and Franz H. Grus[1]

[1]Experimental Ophthalmology, Department of Ophthalmology, University Medical Center of the Johannes Gutenberg University Mainz, Germany
[2]Department of Neuropathology, University Medical Center of the Johannes Gutenberg University Mainz, Germany

Correspondence: Franz H. Grus, Experimental Ophthalmology, Department of Ophthalmology, University Medical Center, Langenbeckstraße 1, 55131 Mainz, Germany; grus@eye-research.org.

Submitted: July 1, 2013
Accepted: December 8, 2013

Citation: Gramlich OW, Lueckner TCS, Kriechbaum M, et al. Dynamics, alterations, and consequences of minimally invasive intraocular pressure elevation in rats. *Invest Ophthalmol Vis Sci*. 2014;55:600–611. DOI: 10.1167/iovs.13-12714

Purpose. An important, yet not exclusive, aspect of primary open angle glaucoma is elevated intraocular pressure (IOP) profiles within fluctuations and pressure peaks. The study aimed at establishing minimally invasive methods for recurrent IOP elevation in rats to investigate the impact of IOP dynamics and pathomorphologic retinal alterations during and after IOP elevation.

Methods. Intraocular pressure was elevated unilaterally in Long Evans rats to a level of ≈35 mm Hg for 1 hour in a total of 30 manipulations within 6 weeks, by using two methods: (1) suction-cup oculopression and (2) loop-adjusted oculopression. Retinal thickness (RT) was measured via optical coherence tomography (OCT), and neuronal survival was analyzed. Additional experiments were performed for "in situ" OCT investigations during exposures to different IOP levels.

Results. A mean IOP exposure of +737.3 ± 9.6 ΔIOP mm Hg for loop adjustment and +188.9 ± 16 ΔIOP mm Hg for suction cup was achieved. Optical coherence tomography examination revealed notable changes of RT between controls, untreated, and treated eyes, and evaluation of neuronal loss showed a significant decrease of retinal ganglion cell (RGC) density in both groups. In situ OCT investigation showed paradoxical retinal distortion and deformation of the optic nerve head toward the eye background.

Conclusions. After accurate IOP elevation with minimally invasive methods, it was possible to detect RGC loss and retinal thinning. While suction cup is capable of simulating accurate arbitrary IOP profiles, loop adjustment enables the detection of pressure-dependent retinal alterations. For the first time, it was feasible to investigate consequences of variable IOP elevation profiles, including pressure peaks, by using real-time live imaging in vivo.

Keywords: recurrent IOP elevation, OCT imaging, retinal degeneration, "in situ" imaging

The pathology of glaucoma is still subject to research. In general, it is considered a multifactorial, heterogeneous group of ocular diseases and is the second most common cause of human blindness worldwide.[1] Furthermore, it is defined by a progressive and irreversible loss of retinal ganglion cells (RGCs) and their axons,[2] which leads to visual field loss in more advanced stages.[3] Glaucoma is often associated with an elevated intraocular pressure (IOP),[4] but solely 60% to 75% of the patients who suffer from primary open angle glaucoma (POAG) show an IOP elevation of more than 21 mm Hg.[5] Several studies have demonstrated that an elevated IOP does not remain at a stable level, but rather that it underlies strong dynamics including IOP fluctuations, pressure peaks, and circadian variations of approximately 10% to 20% (up to ±4 mm Hg).[6–8] Moreover, there are hints of a relationship between IOP fluctuations and increased mean IOP, which further impacts the visual field.[9–12] While half of these studies indicate a direct link to disease progression, others do not. On the other hand, the remaining 25% to 35% of the glaucoma patients suffering from normal tension glaucoma manifest glaucomatous symptoms without significant elevation of the IOP.[13] Nevertheless, an elevated IOP level is still considered a major risk factor. Diagnosing glaucoma is based on anamnesis, IOP measurement, perimetry, and imaging methods. Using optical coherence tomography (OCT) and confocal scanning laser technology, glaucomatous alterations, such as an increase of papillary excavation, bended vessels at the disc margin, decrease of the retinal thickness, and optic disc hemorrhages in 3% to 6% of the cases, can be detected and monitored. As glaucoma is a slow, progressive neurodegenerative disease, already 20% to 40% of the RGCs are irreversibly marred by the time of clinical diagnosis.[14] By now, numerous different hypotheses concerning the pathogenesis exist, but none is sufficient to elucidate the disease pattern on its own. It is assumed that the interaction of individual pathomechanisms, such as IOP-dependent and IOP-independent dysregulations of the ocular blood flow and retinal ischemia, lead to the final loss of RGCs. These pressure-induced dysfunctions and autoregulations in retinal blood vessels often lead to RGC loss by, for example, anoxia and reperfusion injury.[15,16] Currently, there are several methods for inducing invasive and chronic experimental IOP elevations in laboratory animals, such as injection of hypersaline sodium chloride solution into the episcleral vein[17] or its cauterization,[18] injection of microparticles into the anterior chamber,[19]

and laser photocoagulation to the trabecular meshwork.[20] However, these models provide a static IOP elevation, which does not comply with the IOP dynamics in POAG patients and, therefore, a model enabling dynamic IOP adjustments is needed. The first such model reported was that of Joos et al.,[21] who adjusted a loop around the eyeball of a rat in a kind of oculopression for intermittent, short-term, minimally invasive IOP elevation, with a strong potential to conduct arbitrary IOP elevation. Another method based on cup suction oculopression initially described by Ulrich and Ulrich,[22] has been developed for the determination of ophthalmic artery blood pressure in humans and rabbits and might be suitable for arbitrary IOP elevation in rats as well. Therefore, the present study aimed at examining both methods to study a slow, progressive RGC loss model by recurrent short-term IOP elevations and investigated its IOP dynamics during unilateral manipulation. To simulate a variable IOP profile with fluctuations from physiologic IOP to pressure peaks comparable to those of POAG patients, an accumulation of 30 hours of IOP elevation was scheduled for a timespan of 6 weeks. The elevation was performed in rat eyes to an estimated glaucomatous IOP level above 30 mm Hg. The potential glaucomatous effects in the retina, such as thinning of the retinal thickness due to RGC loss, were assessed by OCT and verified by RGC density analysis via Brn3a immunostaining in cross-sections. Enhanced RGC quantification was performed by optic nerve axon counting. As a new and innovative approach, OCT imaging was combined with the loop-adjusted oculopression method described by Joos et al.[21] For the first time, this might offer the possibility of real-time in vivo OCT imaging to investigate alterations of the retinal constitution during IOP pressure changes.

Methods

Animals, IOP Measurements, and Experimental IOP Elevation

Animals. The experiments were approved by the national investigation office in Koblenz, Germany, and the animals were treated in accordance with the ARVO Statement for the Use of Animals in Ophthalmic and Vision Research. Eight-week old male Long Evans rats (Charles River, Sulzfeld, Germany) were maintained in climate-controlled rooms with 12-hour light–dark cycle and fed ad libitum. After the final in vivo experiments, the animals were euthanized by CO_2 fumes, and final cardiac blood was withdrawn, followed by cardiac perfusion with 4% paraformaldehyde/heparin (2000 U/L) solution (Roth, Karlsruhe, Germany).

Minimally Invasive Short-Term IOP Elevation and Study Design. For IOP manipulation, all animals were sedated by using medetomidine (0.185 mL/kg, intramuscular, Dorbene vet; Pfizer, New York, NY). Left eyes (OS) served as control eyes and were moistened continuously with carbomer (ThiloTears; Alcon, Hünenberg, Germany) during the manipulation of the right eyes (OD), which were treated with oxybuprocain (Novesine 0.4%; OmniVision, Puchheim, Germany). After manipulation, both eyes were covered with dexpanthenol (Bepanthen; Bayer, Leverkusen, Germany).

Intraocular pressure elevation was induced in the right eyes by loop-adjusted oculopression (LAOP) in 12 animals as described earlier.[21] Briefly, a silicone loop was tightened around the bulbus to the desired IOP level of 35 mm Hg. The IOP elevation by cup-suction oculopression (CSOP) in another 12 animals is based on sucking the cornea into a cup maintained by a hydrostatic device; herewith the range of the eyeball is reduced and consequently the IOP rises.[22] A silicone cup with 0.4-cm diameter (Timmer Pneumatik, Neuenkirchen, Germany) was used and connected with perfusor lines and several three-way valves (both Braun, Melsungen, Germany) to a hydrostatic mercury column coupled with a 50-mL syringe (Fig. 1). In total, 30 recurrent unilateral IOP elevations, applied for 1 hour in a range of 30 to 35 mm Hg within a period of 6 weeks, were scheduled for both methods.

To identify possible contralateral impacts due to the unilateral IOP elevation, 12 eyes of healthy rats of the same age served as the control group (CTRL). Control animals underwent IOP recording, OCT examination, as well as RGC evaluation and optic nerve axon analysis. Controlled psychologic (handling by examiners, routine investigations on behavior, etc) and physiologic stress (anesthesia procedures on days before IOP recordings, routine exercises) was simulated in controls to ensure comparable stress levels as in the treated groups.

Calibration Study. Simultaneously to the key animal experiments, the CSOP method needed additional validation to examine whether IOP elevation correlates linearly to the applied negative pressure level, as Stodtmeister et al.[23] have proposed. Furthermore, we investigated whether the IOP remained stable or if dynamic IOP changes occurred during the manipulation. Nine rats underwent unilateral IOP elevations at five different negative pressure levels: −100, −200, −300, −400, and −500 mm Hg. Each level was applied for 1 hour and IOP was measured every 5 minutes. The study started with the lowest negative pressure level, and animals were given a pause of 2 days between the next assessments.

IOP Measurements. Intraocular pressure was measured routinely with the TonoLab tonometer (icare, Espoo, Finland) in awake rats between 9 and 12 AM, before IOP elevation (baseline); 2, 4, and 6 weeks after first IOP elevation; and 1 day before euthanasia (end). Furthermore, IOP was assessed in sedated animals before, during, and after IOP manipulation. The mean of 10 consecutive measurements was calculated for each analysis per eye and time point.

Imaging for Glaucomatous-Like Alterations Using Spectral-Domain (SD)–OCT

OCT Setup. Retinae were evaluated by using SD-OCT (Spectralis OCT; Heidelberg Engineering, Heidelberg, Germany). Several changes of the OCT setup, as given by Guo et al.,[24] were needed to enable investigations in rodents, and parameters were standardized throughout all examinations as follows: (1) the OCT device was set to 15.25 diopters, (2) the corneal radius was experimentally determined to 2.75 mm prior, (3) the reference arm was adjusted and fixed at 20500, (4) high-resolution imaging was selected, (5) pattern size was determined to 20° × 15°, which equates to 2.4 mm of X-size and 1.9 mm of Z-size, and (6) ART = 30 frames. To minimize light scattering and to enhance the sharpness of the images, pupils were dilated with tropicamide (Mydriaticum; Pharma Stulln, Stulln, Germany) and eyes were kept moistened with hyaluronic acid (Artelac Splash; Bausch+Lomb, Rochester, NY).

Assessment of the Retinal Thickness. Six weeks after the first IOP elevation, the retinal thickness (RT) around the optic nerve head (ONH) was assessed 2 days after the last IOP elevation and 1 day before euthanasia. In accordance with Guo et al.,[24] our raster scanning pattern consisted of 19 grids with a distance of ±100 μm in between. The central 10th grid was centered on the middle of the ONH. Images were acquired from left and right retinae, and RT was measured from the border of the nerve fiber layer to the end of the outer segment of the photoreceptor layer at ×400 magnification. Three measurements were taken at ±700-, ±800-, and ±900-μm distance to the ONH in the nasal (N) and temporal (T)

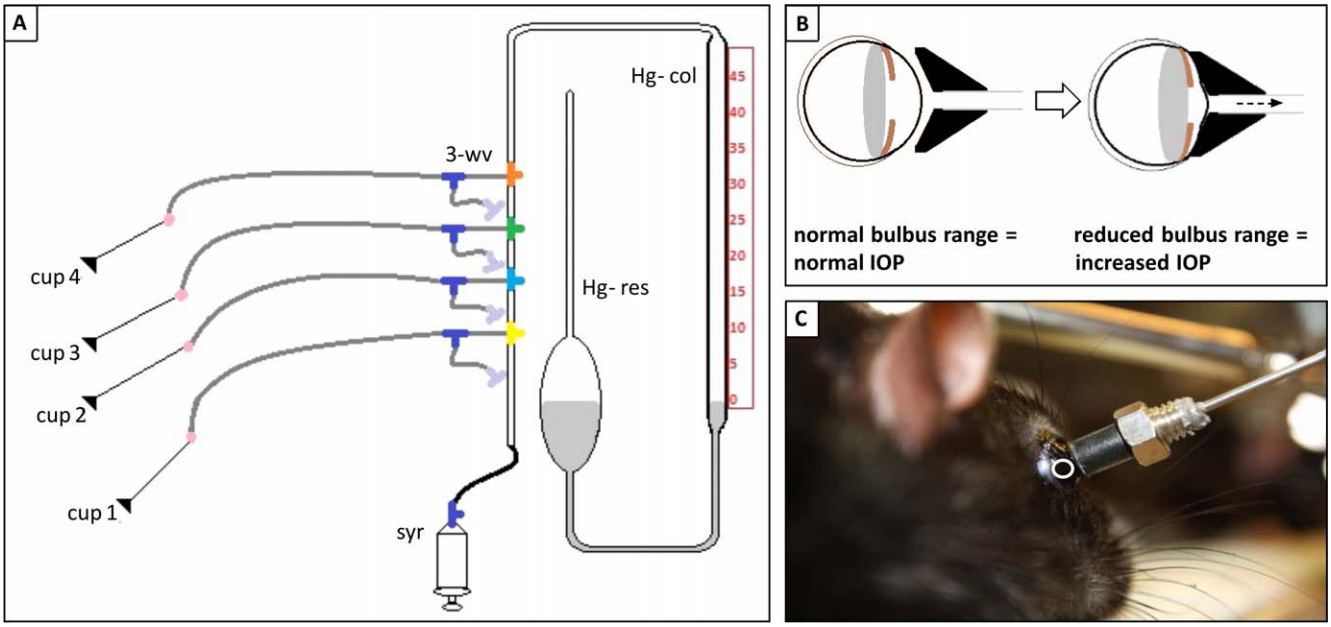

FIGURE 1. Suction-cup oculopression. (**A**) The hydrostatic device consisting of a mercury reservoir (Hg-res) connected to a scaled mercury column (Hg-col) was used to generate a negative pressure level with a perfusor syringe (syr). Four silicone cups were queued in the system via three-way valves (3-wv) that allowed an individual IOP elevation in up to four different animals simultaneously. (**B**) As the cornea and sclera are flexible, but not stretchable, structures, IOP elevation is generally based on the reduction of the bulbus range by sucking the cornea into a cup (Ø, 0.4 cm). (**C**) Attached cup on a rat eye. The *circle* indicates the area for IOP measurement using the TonoLab.

directions, which corresponds to the 10th grid (sinistral or dexter), as well as inferior (I) at 1st, 2nd, and 3rd grid, and superior (S) at the 17th, 18th, and 19th grids (Figs. 4A, 4B).

Pressure-Dependent Retinal Alterations by OCT in In Vivo Real-Time Imaging. To approve an OCT approach to detect pressure-dependent retinal alterations in real-time while the vascular loop was adjusted, three rats were used. Fluctuating IOP pattern was applied in a wave-like IOP profile: 45 mm Hg for 29 minutes → release of the loop for 1 minute; IOP decrease to normal levels → IOP increase to 30 mm Hg for 30 minutes → release of the loop; IOP decrease to normal levels. Retinal thickness was measured correspondingly to the IOP changes before and during the loop manipulation. Afterwards, additional OCT examinations were performed with these preconditioned animals at different IOP levels of 35, 45, and 55 mm Hg to investigate mechanical alterations.

RGC Counts, Axonal Damage Grading, and Analysis of Optic Nerve Axon Density

Brn3a Immunostaining in Retinal Cross-Sections. Eyes were marked to ensure nasotemporally oriented cross-sections and then enucleated, immersions were fixed in 4% paraformaldehyde and paraffin embedded by using a routine protocol. Nasotemporal 10-µm cross-sections were sliced through the ONH for a comparison between the retinal thickness evaluated by OCT and the RGC density in the same retinal axis.

Brn3a is a suitable marker for RGC quantification[25] and Brn3a immunostaining was performed in retinal cross-sections. Briefly, after antigen retrieval in DAKO's Target retrieval solution (95°C, 40 minutes; DAKO, Hamburg, Germany) and blocking, a primary antibody goat anti-Brn3a (C20; Santa Cruz Biotechnology, Santa Cruz, CA) and secondary antibody rabbit anti-goat IgG (P0449, DAKO), labeled with horseradish peroxidase, were used. Visualization was made with 3,3′-diaminobenzidin (DAB; DCS diagnostics, Hamburg, Germany) and routine hematoxylin (Merck, Darmstadt, Germany) counterstaining followed (Fig. 4G). Brn3a-positive cells were counted by using ×40 magnification and a Vanox T microscope (Olympus, Hamburg, Germany) and set in relation to the retinal length (Brn3a cells per mm).[26,27] Retinal ganglion cell density was calculated in five nasotemporally oriented cross-sections per eye.

Optic Nerve Axon Damage and Density. Optic nerves were fixed in 3% glutaraldehyde (Merck) in 0.1 M sodium cacodylate buffer, washed in cacodylate buffer (pH 7.3), thereafter incubated with 1% osmium tetraoxide for 2 hours and dehydrated. After embedding in epoxy resin, semithin transverse sections of the optic nerves were cut at 0.7 µm with a glass knife, using an ultramicrotome (Leica, Solms, Germany), and stained with paraphenylenediamine (PPD). From each optic nerve, up to 15 images were taken at ×100 magnification in a standardized crosswise procedure, representing 25% of the total area of the optic nerve cross-section. As previously described by Ding et al.,[28] optic nerve damage was categorized by using a 5-point damage grading scale, representing degree of damage as follows: grade 1 = healthy optic nerve with no or only very few damaged axons, no gliosis; grade 2 = very mild damage, no gliosis; grade 3 = mild damage with frequent PPD-stained axons; grade 4 = severe damage with many PPD-stained axons and gliotic indications; and grade 5 = severe damage with frequent damaged axons and gliotic areas.[28] Examples of these PPD-stained cross-sections and grades are shown in Figure 5A. The number of axons in all images were assigned automatically with ImageJ software (National Institutes of Health, Bethesda, MD) using a customized macro including standardized threshold setting and the free available particle analyzer. Axon density in an area of 0.05 mm^2 (number of axons per 0.05 mm^2) was calculated in each optic nerve.

Statistical Analysis

Intraocular Pressure. For routine IOP recordings, IOP values of each eye, animal, and time point were analyzed.

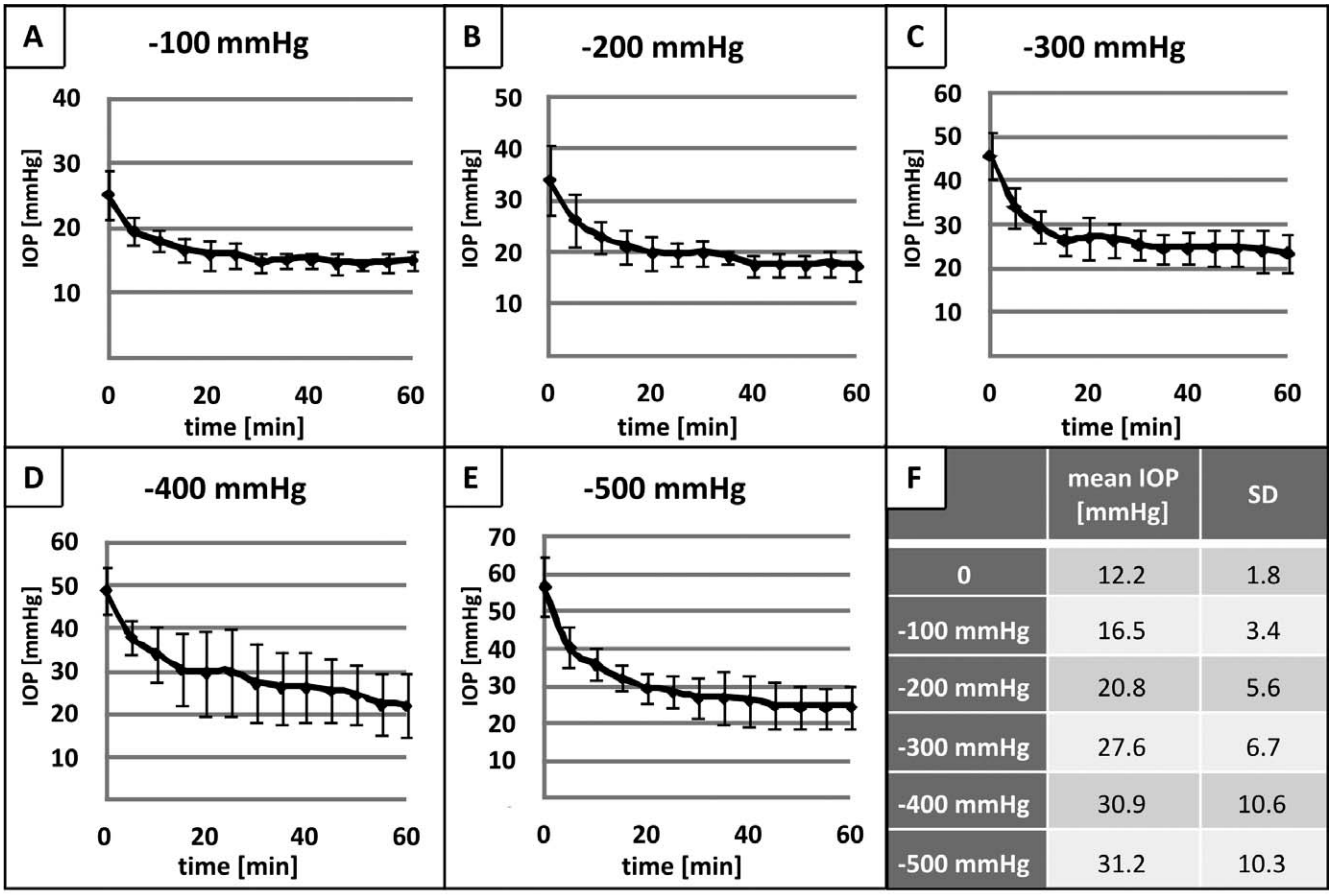

F	mean IOP [mmHg]	SD
0	12.2	1.8
-100 mmHg	16.5	3.4
-200 mmHg	20.8	5.6
-300 mmHg	27.6	6.7
-400 mmHg	30.9	10.6
-500 mmHg	31.2	10.3

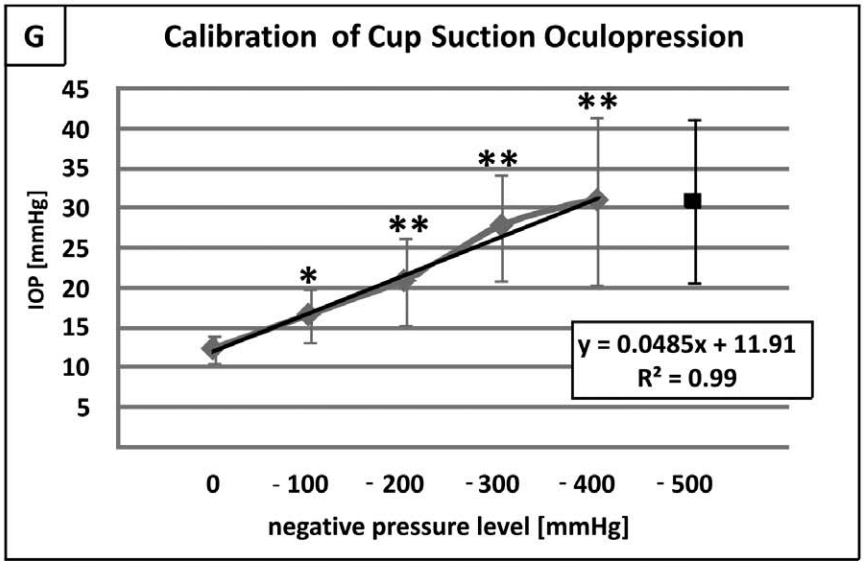

Figure 2. Dynamics, calibration, and elevation of IOP in vivo. (**A**–**E**) After applying negative pressure levels ranging from −100 (**A**) to −500 (**E**) mm Hg to increase IOP in vivo, measurement periods of 5 minutes within a 1-hour period showed continuous decreases with hyperbolic trends. (**F**) Mean values with SD are given in the table. (**G**) The IOP elevation from 12.2 ± 1.8 mm Hg at baseline to 16.5 ± 3.4 mm Hg at −100 mm Hg negative pressure showed a significant increase ($P = 0.02$). Further pressure elevation to −200 mm Hg led to a significant IOP elevation to 20.8 ± 5.6 mm Hg ($P < 0.01$). Comparing −200 to −300 mm Hg, the IOP was elevated again to 27.6 ± 6.7 mm Hg ($P < 0.01$). Elevation to −400 mm Hg revealed further significant increase of the IOP to 30.9 ± 10.6 mm Hg ($P = 0.01$). Exertion of −500 mm Hg did not lead to significant IOP elevation. A *straight calibration line* could be generated, as IOP values are linear for each elevation until −400 mm Hg, related to the corresponding negative pressure level with $y = 0.0485x + 11.91$ and an excellent R^2 value of 0.99. $^{*}P < 0.05$, $^{**}P < 0.01$.

In accordance with Biermann et al.,[29] the cumulative IOP exposure during the IOP elevation was calculated as the $\sum$ of integrated areas under the curve (ΔIOP mm Hg) of each animal after IOP values of the contralateral, untreated eye were subtracted.

In the calibration experiments, a mean IOP for each of the five different negative pressure levels was calculated. To illustrate the dynamics of the IOP during the calibration experiment, data for every measuring period were averaged per negative pressure level.

Integral calculus, regression analyses, and exponential and linear trend lines were prepared in Excel (Microsoft, Redmond, WA). Statistical evaluation was performed with Statistica (StatSoft, Tulsa, OK).

Retinal Thickness, RGC, and Axon Density. Retinal thickness measurement and RGC analysis were performed twice by two independent observers masked to the protocol to ensure reproducibility. Data underwent normal distribution analysis. The three values of the RT measured in each direction were averaged per eye. To detect differences between treated, contralateral, and control eyes, the mean RT was summarized by all quadrants and the mean RTs in the inferior–superior axis and the nasotemporal axis were analyzed. The RGC density in the nasotemporal axis was calculated by averaging the values of Brn3a cells per mm of five cross-sections each eye. Accuracy of the automated axon counting was verified manually on a random basis (sample size: 10% of all images, two observers), revealing an excellent detection, and data were proofed for normal distribution.

Tests. For multiple test schemes, Tukey's honestly significant difference post hoc tests were used. P values < 0.05 were considered as significant. All data are given as mean ± standard deviation (SD).

Results

Experimental Unilateral IOP Elevation in Rats

In general, both minimally invasive methods revealed to be suitable for arbitrary IOP elevation in a range of 30 to 35 mm Hg in rats.

In the calibration experiment for the CSOP method, the mean IOP was determined to be 12.2 ± 1.8 mm Hg at baseline. Exertion of the pressure levels at −100, −200, −300, and −400 mm Hg effected significant elevation of the IOP each time ($P <$ 0.05, Figs. 2A–D). Exertion of −500 mm Hg did not provoke further significant IOP elevation (31.2 ± 10.3 mm Hg, $P =$ 0.99) and indicated the limit of the used cup (Fig. 2E). Regression analysis revealed a linear relation between negative pressure levels (until −400 mm Hg) and IOP increase (Fig. 2G).

Corneal opacities, such as corneal hemorrhages, were observed in all manipulated eyes of the CSOP group and one animal showed a cloudy, cataract-like lens. Paradoxically, there was also spontaneous minimal corneal blurring in left, untreated eyes in four animals. Consequently, the experiment was paused, and the eyes of all CSOP rats fully recovered after dexpanthenol treatment within 1 week. Owing to those unexpected complications, only 10 of 30 scheduled IOP elevations could be performed that led to a cumulative mean IOP exposure of +188.9 ± 16 ΔIOP mm Hg. Side effects due to the loop manipulation were not observed in the LAOP group. A cumulative mean IOP exposure of +737.3 ± 9.6 ΔIOP mm Hg was achieved by 30 LAOP elevations (Fig. 3A).

Routine Monitoring of the IOP in Awake Rats

In both methods, IOP levels were observed in awake rats, between 13.3 ± 1.3 mm Hg (OS) and 13.7 ± 2.1 mm Hg (OD) at baseline and a maximum of 22.8 ± 2.5 mm Hg (OS) and 22.4 ± 2.5 mm Hg (OD). The IOP of the control group ranged between 13.6 ± 1.8 mm Hg at baseline and 17.1 ± 1.7 mm Hg in the course of the study. These data indicate the occurrence of not only increasing IOP levels but also higher IOP fluctuations in awake animals in both experimental groups in comparison to control group. Detailed IOP data are given in Figures 3B and 3C.

Retinal Thickness and Live Imaging Using Spectralis OCT

No significant difference of the mean RT could be identified between contralateral and manipulated eye of the CSOP group in all quadrants (OS: 185.3 ± 11.7 μm, OD: 184.8 ± 10 μm; $P =$ 0.8), or in the inferior–superior axis (OS: 186.3 ± 10.0 μm, OD: 186.3 ± 10.6 μm; $P = 0.9$) and the nasotemporal axis (OS: 183.1 ± 9.8 μm, OD: 183.6 ± 12.4 μm; $P = 0.8$). However, in comparison to the control group, the mean RT in all quadrants of contralateral and manipulated CSOP eyes was significantly thinner (CTRL: 189.3 ± 9.3 μm, CSOP OS: 184.8 ± 10 μm, CSOP OD: 185.3 ± 11.7 μm; $P < 0.01$). These observations continued in axial analysis, where RT of controls in the inferior–superior axis was 187.2 ± 9.8 μm and in the nasotemporal direction, 191.5 ± 8.2 μm. Therefore, inferior–superior RT in CSOP was slightly decreased, and RT in the nasotemporal axis was significantly thinner ($P < 0.01$, Fig. 4C). In the LAOP group, the mean RT in the treated eye was notably decreased, with a mean RT of 191.2 ± 10.8 μm compared to the contralateral mean RT of 193.9 ± 9.8 μm in all quadrants ($P =$ 0.08). This effect was also found when analyzing the RT in the nasotemporal axis, with 191.2 ± 8.8 μm in the manipulated retina compared to 193.9 ± 8.2 μm in the contralateral retina ($P = 0.1$). In the inferior–superior axis, the mean RT was slightly decreased in OD (191.6 ± 12.4 μm) compared to the RT in OS (193.8 ± 11.1 μm, $P = 0.35$). It is conspicuous that the RT in the LAOP group was found to be significantly thicker as in the CSOP group ($P < 0.01$). Furthermore, the RT in all quadrants of the untreated eyes in LAOP animals was even significantly thicker compared to the controls (CTRL: 189.3 ± 9.3 μm, LAOP OS: 193.9 ± 8.2 μm; $P =$ 0.01). This trend was also seen in the axial analysis, but a significant increase was only notable in the inferior–superior axis of untreated retinae in LAOP animals ($P = 0.01$, Fig. 4E).

The OCT approach was suitable to detect pressure-dependent retinal alterations, such as horizontal stretching and vertical impacts, during LAOP performance. Surprisingly, in vivo real-time imaging showed a dynamic RT increase during LAOP manipulation, which was related to the applied IOP (Fig. 6).

Retinal Morphology and RGC Density in Nasotemporal Cross-Sections

The histologic evaluation of the CSOP animals proved an evident, but not significant, loss of RGCs in the nasotemporal axis of treated eyes, as there were 58.1 ± 3.6 Brn3a cells per mm compared to 65.4 ± 9.8 Brn3a cells per mm in contralateral eyes ($P = 0.26$, Fig. 4D). Despite little manipulation time, the data demonstrate 11% fewer RGCs after 10 IOP elevations. It is notable that RGC densities in both eyes of CSOP animals were found to be significantly decreased as compared to a density of 92.0 ± 9.0 Brn3a cells per mm in controls ($P < 0.01$, Fig. 4D).

In comparison, a loss of 12% after 30 IOP elevations was observed in LAOP. This loss was statistically significant with 84.1 ± 9.2 Brn3a cells per mm in the untreated eyes compared to 74.2 ± 8.3 Brn3a cells per mm in manipulated eyes ($P =$

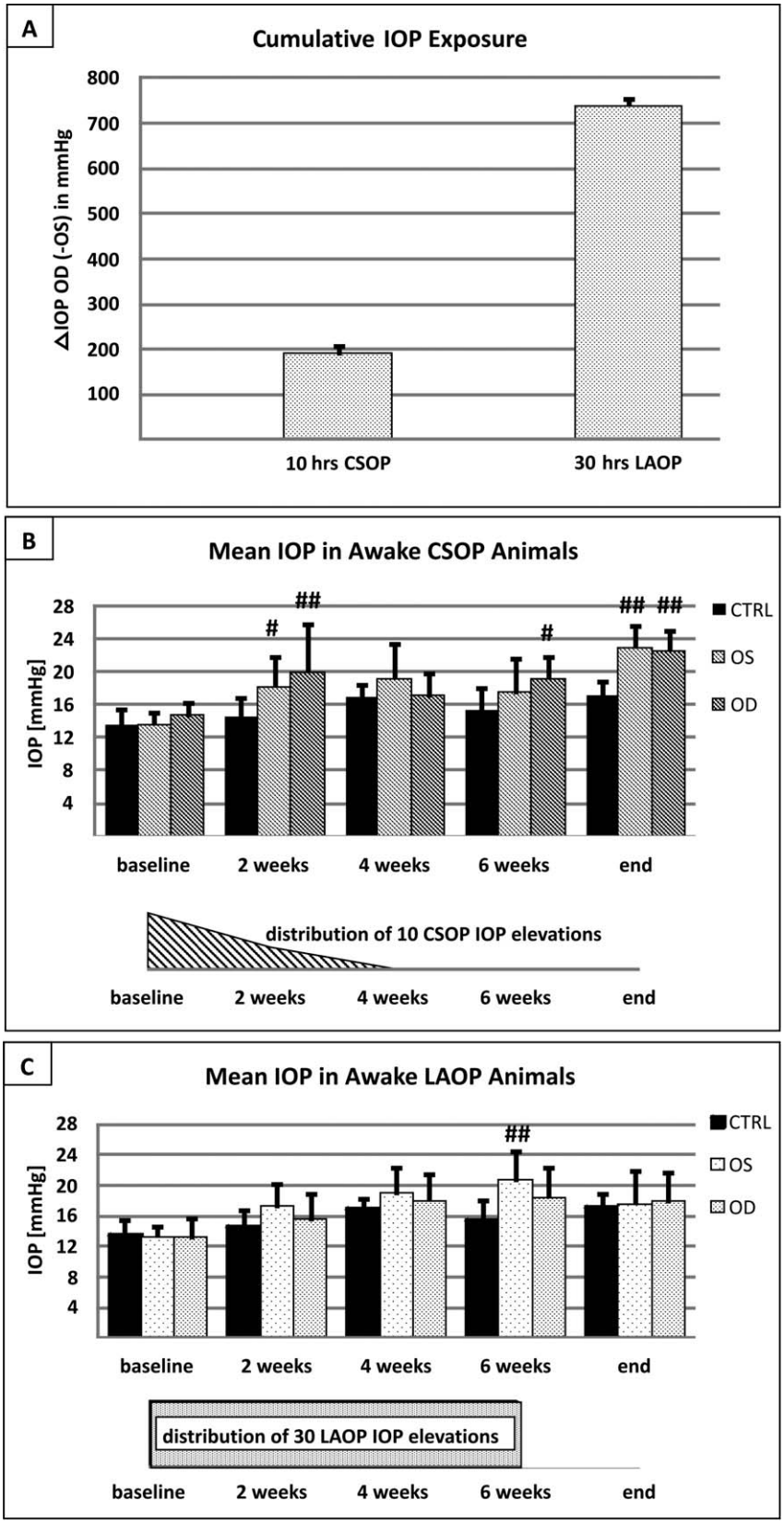

Figure 3. Intraocular pressure exposure and routine IOP recording in awake animals. (**A**) The cumulative mean IOP exposure in the manipulated right eyes was calculated as ΔIOP mm Hg exposure on the *abscissa*, as the difference between IOP values of the manipulated (OD) and contralateral (OS) eye. Ten hours of IOP elevations using CSOP led to a cumulative IOP exposure of 188.9 ± 16 ΔIOP mm Hg. In the LAOP group, the cumulative IOP during 30 IOP elevations (30 h) was 737.3 ± 9.6 ΔIOP mm Hg. (**B**) In the CSOP group, a significant elevation of the physiologic IOP at different time points was identified not only in manipulated eyes but also in contralateral eyes compared to control group. The latter was determined to be

13.6 ± 1.8 mm Hg (CTRL) with 13.5 ± 1.4 mm Hg in OS and 14.6 ± 1.6 mm Hg in OD in animals at baseline before CSOP IOP manipulation started. After 2 weeks of manipulation, the IOP was significantly elevated to 18.1 ± 3.6 mm Hg in OS ($P = 0.02$) and to 19.9 ± 5.7 mm Hg in OD ($P < 0.01$) compared to 14.5 ± 2.1 mm Hg in controls. The IOP of the CSOP group fluctuated in the subsequent weeks and reached a significantly elevated IOP level at the end point with 22.9 ± 2.6 mm Hg in OS ($P < 0.01$) and 22.4 ± 2.4 mm Hg in OD ($P < 0.01$) compared to 17.1 ± 1.7 mm Hg in control eyes. The CSOP group underwent 10 experimental IOP elevations, which took place within the first 2 weeks, as shown below the *abscissa* in the distribution of CSOP IOP elevations. (**C**) Animals of the LAOP group showed a fluctuating IOP pattern throughout the study. Before IOP manipulation started using LAOP, baseline values revealed IOP levels of 13.6 ± 1.8 mm Hg in the control group and 13.2 ± 1.4 mm Hg in OS and 13.0 ± 2.5 mm Hg in OD of the LAOP group. In contrast to the CSOP group, only contralateral eyes were significantly elevated after 6 weeks (CTRL: 15.4 ± 2.5 mm Hg, OS: 20.6 ± 3.8 mm Hg, $P < 0.01$, OD: 18.3 ± 4.0 mm Hg) compared to the control group. LAOP IOP elevations were performed continuously during 6 weeks as shown below the *abscissa*. Significances compared to controls at the same time points are marked as #. #$P < 0.05$, ##$P < 0.01$.

0.03, Fig. 4F). Furthermore, no changes in the RGC densities were determined between the untreated eyes of LAOP animals and controls, but a significant decrease of RGCs was found in retinae after IOP exposures ($P = 0.01$, Fig. 4F).

Morphologic changes in the Brn3a-stained cross-sections, indicating acute pathogenetic effects, were not observed in any retinae. Furthermore, the retinal architecture in the nasotemporal axis seemed intact 6 weeks after the first IOP elevation and was in accordance with the observations during OCT imaging (Fig. 4G).

Grade of Axonal Damage and Axon Density in the Optic Nerves

Analysis of the grading revealed increased axonal damage in the optic nerves of eyes exposed to IOP elevation. After applying a 5-point damage grading scale, whereby grade 1 represents healthy axons and grade 5 represents severe damage, the mean grade of degeneration in the optic nerves was 2.0 ± 0.3 in OS versus 2.7 ± 0.5 in OD ($P < 0.01$) in the CSOP group and 1.6 ± 0.2 in OS versus 2.2 ± 0.2 in OD ($P < 0.01$) in LAOP animals. The data indicate a significant increase of axonal damage in the manipulated eyes 6 weeks after the first intermittent IOP elevation in comparison to the untreated, contralateral eye as well as to a grade of 1.5 ± 0.2 ($P < 0.01$) in control optic nerves (Fig. 5C).

The result of the axon density analysis was comparable to the Brn3a data. In comparison to the axon density in the control group, all animals in the experimental groups showed a significantly decreased number of axons not only in their manipulated eyes but also in their contralateral ones. Controls had 22,528 ± 2127 axons per 0.05 mm^2 and showed no difference with the untreated left eyes in LAOP animals (23,144 ± 1956 axons per 0.05 mm^2), while the untreated eyes of the CSOP group with 21,035 ± 3410 axons per 0.05 mm^2 revealed a slight reduction. Axon density of the manipulated eyes therefore showed a significant decrease of approximately 17% 6 weeks after the first IOP elevation in comparison to the axon density in untreated eyes (CSOP OD: 17,505 ± 2890, $P = 0.02$; LAOP OD: 19,266 ± 2366, $P < 0.01$) and in controls (CTRL versus CSOP OD: $P < 0.01$; CTRL versus LAOP OD: $P = 0.04$). Details of axonal damage and axon density in the optic nerves are given in Figure 5.

Discussion

Both methods worked properly to increase IOP. Results of the calibration study showed linear dependence between negative pressure levels and showed that IOP increase is related to cup size and shape as described for this method.[22,23] Intraocular pressure values using LAOP are basically comparable to the data of Joos et al.,[21] but this method offers opportunities to achieve higher IOP values. Furthermore, both recurrent short-term IOP elevations for a period of 6 weeks elicited significant RGC loss and marked changes of the retinal architecture.

In comparison to static glaucoma animal models, which show high bias in IOP values and result in relatively progressive RGC losses in short durations,[30–32] this short-term recurrent IOP elevation model revealed a slow progression. A RGC loss of approximately 10% in the nasotemporal axis and an axonal loss of approximately 17% within 6 weeks correspond to the human pathology of glaucoma. Its practicability, success rate, as well as its control seem not to be difficult. However, both methods are more or less invasive, concerning the corneal opacities, and are prospectively suitable for simulating complex and arbitrary IOP patterns up to high IOP levels. Both methods have specific advantages and disadvantages, which have to be considered in future studies: our cup caused corneal alterations in lasting utilization, a problem that has to be controlled in the future, and it is limited to a mean IOP level of 31 mm Hg. It turned out that cups with the same diameter but with more acute angles elicited an IOP increase of up to 80 mm Hg; once the cup is calibrated, the accuracy of the method is outstanding and well-controlled pressure changes are realizable (Lueckner T, et al. *IOVS* 2013;54:ARVO E-Abstract 1985). The LAOP method is not as accurate in adjusting the desired IOP increase and needs high practical skills, but it is more suitable for longer-lasting, recurrent elevations without irritations. The major advantage of LAOP is the opportunity for in vivo real-time retinal imaging using OCT devices to investigate pressure-dependent retinal alterations during IOP elevation.

Routine IOP recording revealed increased bilateral IOP in awake rats of the experimental groups throughout the study, while no manipulations were proceeding. Partially, these IOP increases were statistically significant compared to IOP levels of controls. Comparable phenomena were observed in other studies in which an increased degree of optic nerve injury after hypersaline injection was associated with significant higher IOP values.[33]

But it has to be noted that the controls were subjected to similar stress levels as animals undergoing IOP manipulation and responded with a slight IOP increase between baseline and the end of the study. Nevertheless, nearly all recorded IOP values of controls in our study stayed in a physiologic range between a minimum of 8.1 ± 0.7 mm Hg[34] and a maximum of 16.7 ± 2.3 mm Hg,[33] assessed for rats during light phase with the TonoLab. Even a few recurrent IOP elevations elicited prolonged dynamic bilateral IOP regulation, but also IOP levels up to 22.9 ± 2.6 mm Hg were reached in the experimental groups. This leads to the conclusion that stress influences IOP values in healthy animals, but stress combined with intermittent IOP elevations elicit higher IOP values and also higher fluctuations in awake animals. This conclusion reflects aspects of the hypothesis described by Brody et al.,[35] who has stated that in humans, psychologic stress during short-term IOP elevation elicits higher IOP values than the short-term IOP elevation itself. Moreover, there were several hints of bilateral effects after unilateral manipulation, especially in the CSOP group, because the data of OCT investigations, Brn3a

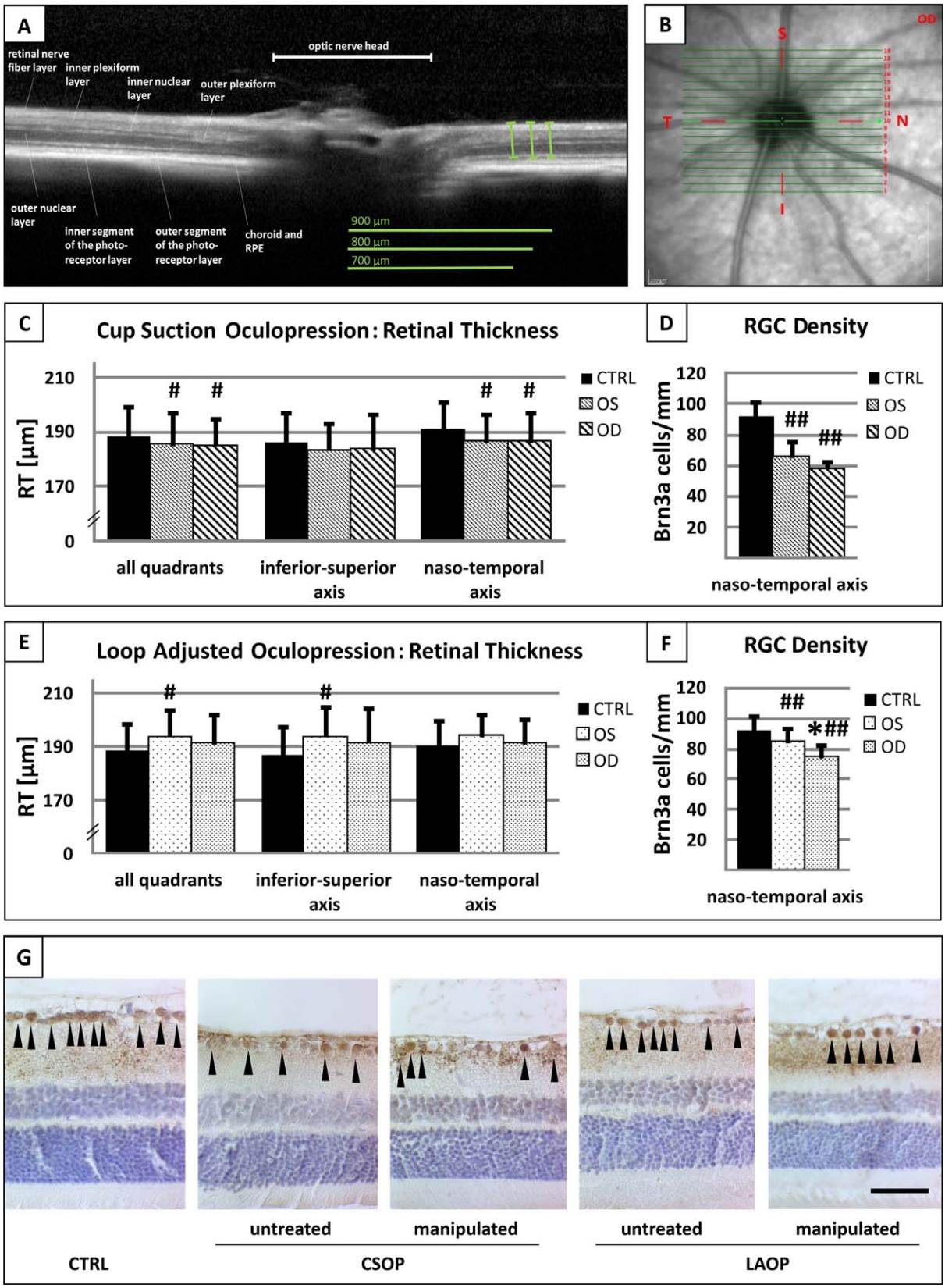

Figure 4. Retinal thickness and RGC density. (**A**) Using Spectralis OCT, a distinct differentiation between the layers of the rat retina can be made (layers labeled according to Guo et al.[24]). The RT was measured from the nerve fiber layer to the most distinctive layer, the outer segment of the photoreceptor layer. (**B**) The RT measurements were done in temporal (*T*), superior (*S*), nasal (*N*), and inferior (*I*) direction at ±700-, ±800- and ±900-µm distance to the optic nerve head. (**C**) After 10 recurrent IOP elevations in the CSOP group, the mean RT (listed on *adjusted ordinate* for better illustration of RT changes) in all quadrants as well as in the nasotemporal axis was significantly decreased in the manipulated and contralateral eye in comparison to the control (CTRL, $P < 0.05$). Interestingly, RT did not differ between the left and the manipulated right eyes, and analysis of

RGC density revealed comparable results. (**D**) Brn3a immunostaining of retinal cross-sections revealed a significant loss of RGCs in both eyes after IOP elevations, compared to the control. Even a more severe, but not significant ($P = 0.26$), loss of RGCs in the nasotemporal axis was observed in eyes (OD) after IOP elevations. (**E**) Examination of the RT in the LAOP group showed a generally thicker retina in both eyes, which was partially significant in comparison to controls. In the LAOP group, the mean RT in all quadrants of the right eyes after 30 IOP elevations was notably, but not significantly, decreased compared to the contralateral left eyes ($P = 0.37$). The detailed analysis of both *axes* confirmed the findings of slight decreases in the treated eyes. (**F**) Thirty recurrent IOP elevations in the right eyes (OD) led to a significant loss of Brn3a cells in the nasotemporal axis in comparison to the contralateral eyes ($P = 0.03$). As for the CSOP group, RGC density was significantly decreased in both eyes against the control and may indicate methodic peculiarities of the IOP elevation techniques with different (bilateral?) impacts. Significances to controls are marked as # and to the contralateral eyes, as *. $\#P < 0.05$, $\#\#P < 0.01$; $^{*}P < 0.05$, $^{**}P < 0.01$. (**G**) The panel gives an overview of the retinal architecture and the RGC density after Brn3a immunostaining in controls (CTRL), untreated, and manipulated eyes of the experimental groups (CSOP/LAOP). Brn3a-positive cells (*triangles*) were distinguishable despite the DAB background. In general, slight reduction of Brn3a-positive cells and retinal thickness (especially in CSOP animals) were observable, while the retinal layers displayed no acute pathologic changes. *Scale bar*: 50 μm.

immunostaining, and IOP measurements were in line: (1) the retinal thickness in both eyes was reduced significantly compared to controls, especially in the nasotemporal axis ($P < 0.05$, Fig. 4C); (2) RGC density in the nasotemporal axis was reduced significantly ($P < 0.01$) and did not differ between treated and untreated eyes (Fig. 4D); and (3) IOP values were elevated, partially significantly ($P < 0.05$), in both eyes in comparison to controls (Fig. 3B). A bilateral sectorial impact using the cup suction method, accompanied by RGC loss in the nasotemporal axis of the untreated retina, might be an explanation for that unexpected observation. Despite the occurrence of heterogeneous labeling, nonspecific DAB

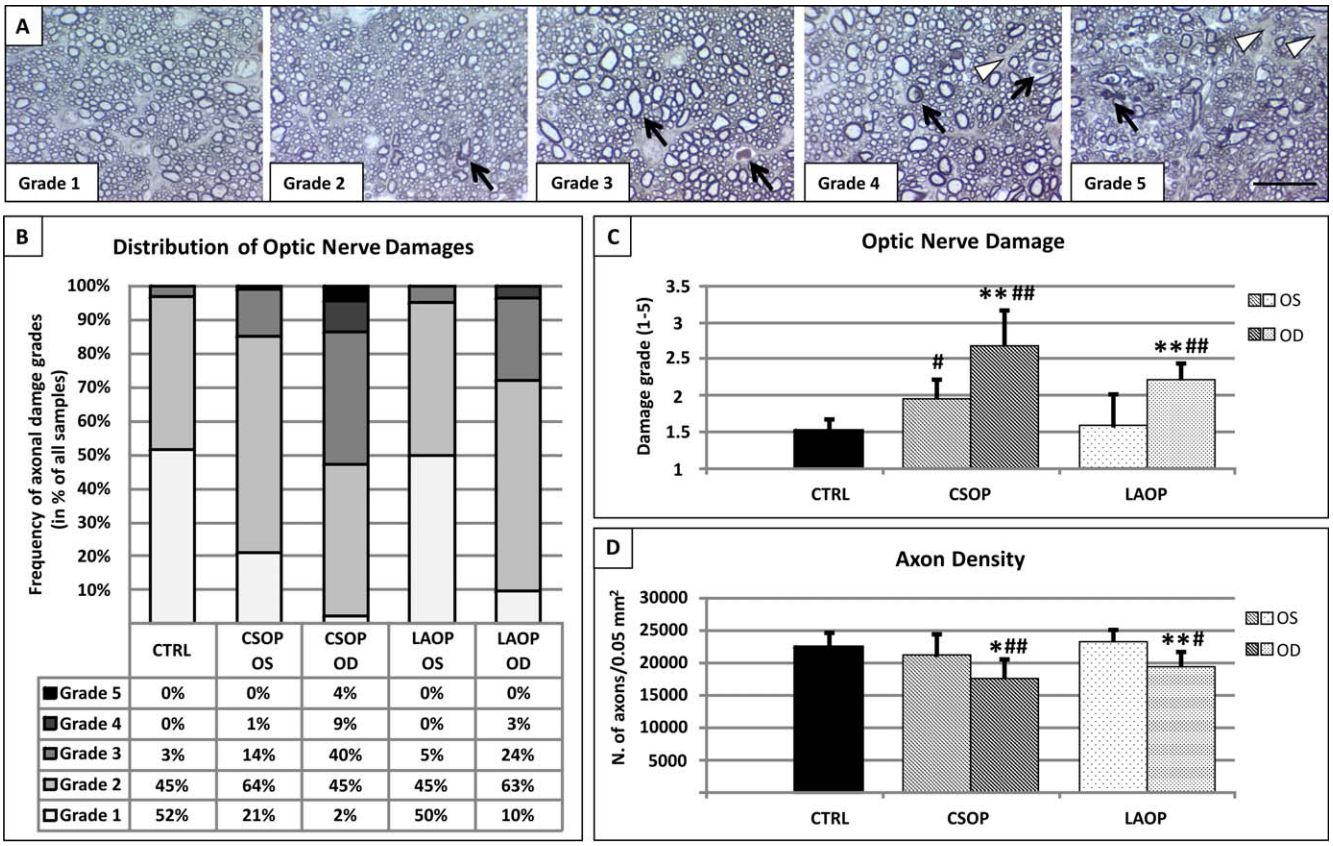

	CTRL	CSOP OS	CSOP OD	LAOP OS	LAOP OD
Grade 5	0%	0%	4%	0%	0%
Grade 4	0%	1%	9%	0%	3%
Grade 3	3%	14%	40%	5%	24%
Grade 2	45%	64%	45%	45%	63%
Grade 1	52%	21%	2%	50%	10%

Figure 5. Evaluation of optic nerve damage. (**A**) The optic nerve damage was determined by using a 5-point damage grading scale according to Ding et al.[28] Each grade represents a different stage of optic nerve damage; grade 1: healthy nerve; grade 2: slight damage with only few damaged axons; grade 3: moderate damage with frequent degenerated axons; grade 4: severe damage with mostly degenerated axons and the appearance of gliotic areas; grade 5: severe axon degeneration in the optic nerve with frequent gliotic areas. Note the appearance of swollen and shrunken axons up to total degeneration (*black arrows*) and gliotic tissue (*white triangle*). *Scale bar*: 20 μm. (**B**) The frequency of axonal damage grades as shown in (**A**) was calculated as the distribution of optic nerve damage. Damage grades of CTRL eyes and contralateral and manipulated eyes of the CSOP and LAOP groups were compared. The highest frequency of grade 1 is shown for CTRL eyes (52%); grade 2 for contralateral eyes of CSOP group (64%); grade 3 (40%), grade 4 (9%), and grade 5 (4%) for treated eyes of the CSOP group. Overall, optic nerves of manipulated eyes from CSOP and LAOP show higher damage grades than optic nerves in contralateral eyes and CTRL eyes. (**C**) The mean optic nerve damage was calculated per group. CTRL and LAOP OS showed almost the same damage grades. Significant differences were identified between contralateral and manipulated eyes of CSOP ($P < 0.01$) and LAOP ($P < 0.01$) groups. Additionally, significantly elevated optic nerve damage was found in manipulated eyes of CSOP ($P < 0.01$) and LAOP ($P < 0.01$) compared to control group. (**D**) The number of axons has been analyzed as axonal density to an area of 0.05 mm^2 in the optic nerves (number of axons per 0.05 mm^2). Here, manipulated eyes from CSOP and LAOP groups show significantly reduced axon density compared to CTRL eyes ($P < 0.01$) as well as when compared to their contralateral eyes (CSOP: $P < 0.05$, LAOP: $P < 0.01$). Significances to controls are marked as # and to the contralateral eyes, as *. $\#P < 0.05$, $\#\#P < 0.01$; $^{*}P < 0.05$, $^{**}P < 0.01$.

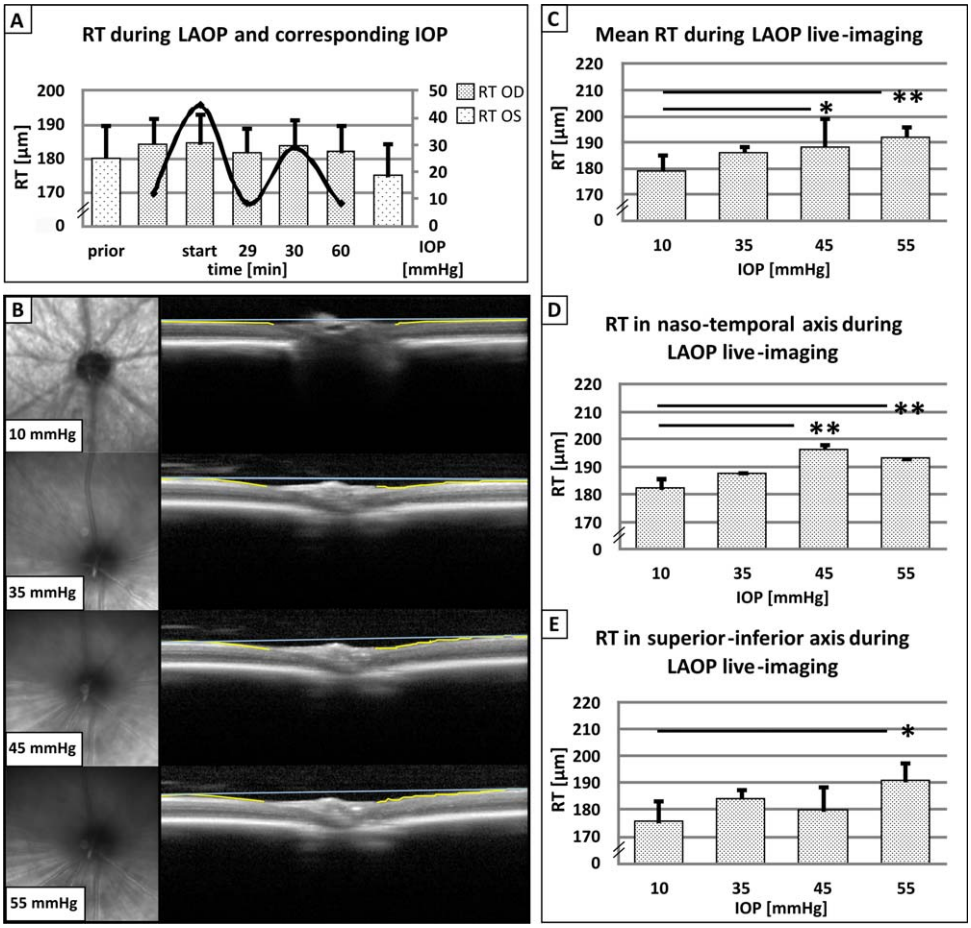

Figure 6. "In situ" pressure-dependent retinal alterations by OCT real-time imaging. (**A**) The application of a wave-like IOP profile (*black line*, IOP in mm Hg, *ordinate right*) during 60 minutes (*abscissa*) resulted in a periodic increase and decrease of the RT in the manipulated eyes, while the RT in the untreated left eyes minimally decreased with time. (**B**) Representative fundi (*left side*) and images of the nasotemporal retinal axis (*right side*) at different IOP levels are given. The ONH formed one line (*grey line*) with the retina in the nasotemporal axis when the retina was at a normal IOP level of 10 mm Hg, and the border of the retinal nerve fiber layer (outlined in *yellow*) appeared nearly planar. The loop was adjusted to a target IOP of 35, 45, and 55 mm Hg. A deformation of the ONH toward the eye background could be observed in the fundus images, which impacts the retinal organization (distortions of the nerve fiber layer, *yellow line*), as shown in the OCT nasotemporal cross-sections. (**C**) The mean RT in all four quadrants in micrometers (*ordinate*) was plotted against the applied IOP and time span (*abscissa*) and increased significantly at 45 mm Hg ($P = 0.02$) and at 55 mm Hg ($P < 0.01$) compared to RT at a baseline IOP of 10 mm Hg. (**D**) Stronger impacts were noticed in the nasotemporal axis, where retinal cross-section appeared to curve in the nasotemporal axis and showed a significant increase in the RT at 45 mm Hg ($P < 0.01$) and 55 mm Hg ($P < 0.01$). (**E**) In the inferior–superior axis, only IOP of 55 mm Hg caused a significant increase in the RT. $^{*}P < 0.05$, $^{**}P < 0.01$.

background in neuronal tissue, and the extreme reliability of accurate slicing, Brn3a immunostaining in retinal cross-sections might not be the best approach for RGC quantification primarily. But in our study it offered the possibility for comparative analysis of the retinal thickness, histologic morphology, and RGC loss in the nasotemporal axis. To deal with the aforementioned problems in our Brn3a immunostainings (Fig. 4G), the common method of optic nerve axon counting was used to assure a reliable RGC quantification. Axonal densities in the optic nerves of controls and untreated eyes of both experimental groups were similar. In contrast, significant axonal damage and axonal losses were determined after exposure to IOP elevations ($P < 0.05$, Figs. 5B–D). Using the CSOP technique, the damage seemed to be more intense after shorter time of intermittent IOP elevations, in comparison to the loop-adjusted method first described by Joos et al.[21] Nevertheless, retinal changes in the nasotemporal axis of the untreated eyes in CSOP were prominent. Whether these changes are linked to methodic peculiarities of the IOP elevation technique, and whether these bilateral effects are substantial and to which extent stress plays a role, needs further clarification in following studies. In summary, using the CSOP method, it is possible to induce glaucomatous-like alterations such as prolonged IOP variability, decrease of the retinal thickness, and significant loss of RGCs even by a few intermittent IOP elevations. This approach further offers the possibility to investigate the impact of wide-ranging controlled single IOP elevations and might be a suitable tool to simulate situations of acute angle closure glaucoma in vivo.

In the present study, significant RT changes, using the OCT device, are lacking behind the time point of significant RGC loss; this shows that the problematic nature of diagnosis in humans is transferred to in vivo investigations. Nevertheless, the OCT device offered many opportunities, but many researchers report high bias in OCT thickness measurements with occasional paradoxical data, using animal models with static IOP elevations. Thus, it has been shown that reliable OCT data are achievable[24] but difficult to obtain, and results have been either sparely or not published, while generally, it is practicable to track retinal changes in rodent models with pressure-independent retinal degenerations.[36–40] Even in our study, CSOP animals displayed signs of a thinning of the retinal

thickness. The opposite was observed in LAOP animals, where the retinal thickness became thicker (Figs. 4C, 4E). To overcome this issue, our OCT imaging method was combined with the technique of loop-adjusted IOP elevation by Joos et al.[21] This new approach was extremely suitable for achieving "in situ" insight into the occurrence of pressure-dependent retinal alterations. With the use of the LAOP technique, retinal impacts were examined at IOP pressure levels of 35, 45, and 55 mm Hg, and preliminary data suggested that the retinal thickness became thicker with increasing IOP levels (Teister J, et al. *IOVS* 2013;54:ARVO E-Abstract 1458). Moreover, marked expansion was observed at 35 mm Hg, which was in accordance with the observations made in the LAOP group of our study, and the increase was statistically significant at the higher IOP levels of 45 and 55 mm Hg (Figs. 6C, 6D). The vertical expansion seemed to be positively linked to the applied pressure level, as our data showed in a wave-like profile between normal IOP values and 35 mm Hg (Fig. 6A). Briefly, the higher the IOP, the thicker was the retina in the present short-term recurrent IOP elevation animal model. Based on our investigations, a horizontal stretching, as well as an increasing vertical expansion of the retina in response to the IOP elevation in vivo, might be offered as an explanation and for further investigation. Therefore, the thinning of the retina, using an OCT device in pressure-related glaucoma animal models, can be interpreted as a surrogate parameter as stated by Guo et al.,[24] but only in consideration of the current IOP value. We further conclude that increase and decrease of the retinal thickness are related to the progression of RGC loss in pressure-related glaucoma animal models. An increase occurred in the loop-adjusted model that could be interpreted as a swelling or edema of the retina in an early-damage stage due to changes of the IOP levels. When these IOP manipulations were paused for a longer time as in our CSOP group, the expected decrease in retinal thickness was observed.

In summary, both methods are suitable for simulating variable and arbitrary selectable IOP profiles in vivo to investigate the impact of IOP dynamics occurring in POAG patients, including IOP fluctuation ranging from normal IOP levels to high pressure peaks. Furthermore, combining the LAOP technique and OCT imaging, it is now possible to investigate real-time pressure-dependent retinal alterations in situ when the IOP is elevated. This innovative approach contributes to the investigation of the role of IOP fluctuation and its impact on the retina in the pathology of glaucoma.

Acknowledgments

Supported by Ernst und Berta Grimmke-Stiftung.

Disclosure: **O.W. Gramlich**, None; **T.C.S. Lueckner**, None; **M. Kriechbaum**, None; **J. Teister**, None; **X. Tao**, None; **H.D. von Pein**, None; **N. Pfeiffer**, None; **F.H. Grus**, None

References

1. Quigley HA, Broman AT. The number of people with glaucoma worldwide in 2010 and 2020. *Br J Ophthalmol*. 2006;90:262–267.
2. EUGS. Introduction chapter. *Terminology and Guidelines for Glaucoma*. European Galucoma Society; 2003:1–13.
3. Duane's O. Duane's Ophthalmology on DVD-ROM Edition 2010. *Clin Exp Optom*. 2010;94:506–507.
4. Pfeiffer N, Krieglstein GK, Wellek S. Knowledge about glaucoma in the unselected population: a German survey. *J Glaucoma*. 2002;11:458–463.
5. Sommer A, Tielsch JM, Katz J, et al. Relationship between intraocular pressure and primary open angle glaucoma among white and black Americans: The Baltimore Eye Survey. *Arch Ophthalmol*. 1991;109:1090–1095.
6. Mansouri K, Shaarawy T. Continuous intraocular pressure monitoring with a wireless ocular telemetry sensor: initial clinical experience in patients with open angle glaucoma. *Br J Ophthalmol*. 2011;95:627–629.
7. Liu JH, Zhang X, Kripke DF, Weinreb RN. Twenty-four-hour intraocular pressure pattern associated with early glaucomatous changes. *Invest Ophthalmol Vis Sci*. 2003;44:1586–1590.
8. Mosaed S, Liu JH, Weinreb RN. Correlation between office and peak nocturnal intraocular pressures in healthy subjects and glaucoma patients. *Am J Ophthalmol*. 2005;139:320–324.
9. Caprioli J, Coleman AL. Intraocular pressure fluctuation a risk factor for visual field progression at low intraocular pressures in the advanced glaucoma intervention study. *Ophthalmology*. 2008;115:1123–1129.e1123.
10. Loukil I, Korchene N, Hachicha F, et al. Ocular risk factors for progression of primary open angle glaucoma in the Tunisian population. *J Fr Ophtalmol*. 2013;36:324–330.
11. Ontario HQ. Diurnal tension curves for assessing the development or progression of glaucoma: an evidence-based analysis. *Ont Health Technol Assess Ser*. 2011;11:1–40.
12. Quaranta L, Katsanos A, Russo A, Riva I. 24-hour intraocular pressure and ocular perfusion pressure in glaucoma. *Surv Ophthalmol*. 2013;58:26–41.
13. Quigley HA. Open-angle glaucoma. *N Engl J Med*. 1993;328:1097–1106.
14. Guo L, Cordeiro MF. Assessment of neuroprotection in the retina with DARC. *Prog Brain Res*. 2008;173:437–450.
15. Flammer J, Orgul S. Optic nerve blood-flow abnormalities in glaucoma. *Prog Retin Eye Res*. 1998;17:267–289.
16. Flammer J, Orgul S, Costa VP, et al. The impact of ocular blood flow in glaucoma. *Prog Retin Eye Res*. 2002;21:359–393.
17. Morrison JC, Moore CG, Deppmeier LM, Gold BG, Meshul CK, Johnson EC. A rat model of chronic pressure-induced optic nerve damage. *Exp Eye Res*. 1997;64:85–96.
18. Shareef SR, Garcia-Valenzuela E, Salierno A, Walsh J, Sharma SC. Chronic ocular hypertension following episcleral venous occlusion in rats. *Exp Eye Res*. 1995;61:379–382.
19. Sappington RM, Carlson BJ, Crish SD, Calkins DJ. The microbead occlusion model: a paradigm for induced ocular hypertension in rats and mice. *Invest Ophthalmol Vis Sci*. 2010;51:207–216.
20. WoldeMussie E, Ruiz G, Wijono M, Wheeler LA. Neuroprotection of retinal ganglion cells by brimonidine in rats with laser-induced chronic ocular hypertension. *Invest Ophthalmol Vis Sci*. 2001;42:2849–2855.
21. Joos KM, Li C, Sappington RM. Morphometric changes in the rat optic nerve following short-term intermittent elevations in intraocular pressure. *Invest Ophthalmol Vis Sci*. 2010;51:6431–6440.
22. Ulrich WD, Ulrich C. Oculo-oscillodynamography, a new procedure for the determination of ophthalmic artery blood pressure and ocular pulse curve analysis [in German]. *Klin Monbl Augenheilkd*. 1985;186:385–388.
23. Stodtmeister R, Pillunat L, Mattern A, Polly E. Relation of negative pressure difference and artificially elevated intraocular pressure using the suction cup method [in German]. *Klin Monbl Augenheilkd*. 1989;194:178–183.
24. Guo L, Normando EM, Nizari S, Lara D, Cordeiro MF. Tracking longitudinal retinal changes in experimental ocular hypertension using the cSLO and spectral domain-OCT. *Invest Ophthalmol Vis Sci*. 2010;51:6504–6513.
25. Nadal-Nicolas FM, Jimenez-Lopez M, Sobrado-Calvo P, et al. Brn3a as a marker of retinal ganglion cells: qualitative and quantitative time course studies in naive and optic nerve-

injured retinas. *Invest Ophthalmol Vis Sci*. 2009;50:3860–3868.

26. Ittner LM, Wurdak H, Schwerdtfeger K, et al. Compound developmental eye disorders following inactivation of TGFbeta signaling in neural-crest stem cells. *J Biol*. 2005;4:11.
27. Dorfman D, Fernandez DC, Chianelli M, Miranda M, Aranda ML, Rosenstein RE. Post-ischemic environmental enrichment protects the retina from ischemic damage in adult rats. *Exp Neurol*. 2013;240:146–156.
28. Ding QJ, Cook AC, Dumitrescu AV, Kuehn MH. Lack of immunoglobulins does not prevent C1q binding to RGC and does not alter the progression of experimental glaucoma. *Invest Ophthalmol Vis Sci*. 2012;53:6370–6377.
29. Biermann J, van Oterendorp C, Stoykow C, et al. Evaluation of intraocular pressure elevation in a modified laser-induced glaucoma rat model. *Exp Eye Res*. 2012;104:7–14.
30. Bouhenni RA, Dunmire J, Sewell A, Edward DP. Animal models of glaucoma. *J Biomed Biotechnol*. 2012;2012:692609.
31. Vidal-Sanz M, Salinas-Navarro M, Nadal-Nicolas FM, et al. Understanding glaucomatous damage: anatomical and functional data from ocular hypertensive rodent retinas. *Prog Retin Eye Res*. 2011;31:1–27.
32. Goldblum D, Mittag T. Prospects for relevant glaucoma models with retinal ganglion cell damage in the rodent eye. *Vision Res*. 2002;42:471–478.
33. Morrison JC, Jia L, Cepurna W, Guo Y, Johnson E. Reliability and sensitivity of the TonoLab rebound tonometer in awake Brown Norway rats. *Invest Ophthalmol Vis Sci*. 2009;50:2802–2808.
34. Ohashi M, Aihara M, Saeki T, Araie M. Efficacy of TonoLab in detecting physiological and pharmacological changes in rat intraocular pressure: comparison of TonoPen and microneedle manometry. *Jpn J Ophthalmol*. 2008;52:399–403.
35. Brody S, Erb C, Veit R, Rau H. Intraocular pressure changes: the influence of psychological stress and the Valsalva maneuver. *Biol Psychol*. 1999;51:43–57.
36. Fischer MD, Huber G, Paquet-Durand F, et al. In vivo assessment of rodent retinal structure using spectral domain optical coherence tomography. *Adv Exp Med Biol*. 2012;723:489–494.
37. Kim KH, Puoris'haag M, Maguluri GN, et al. Monitoring mouse retinal degeneration with high-resolution spectral-domain optical coherence tomography. *J Vis*. 2008;817;11–11.
38. Xu J, Molday LL, Molday RS, Sarunic MV. In vivo imaging of the mouse model of X-linked juvenile retinoschisis with fourier domain optical coherence tomography. *Invest Ophthalmol Vis Sci*. 2009;50:2989–2993.
39. Gabriele ML, Ishikawa H, Schuman JS, et al. Optic nerve crush mice followed longitudinally with spectral domain optical coherence tomography. *Invest Ophthalmol Vis Sci*. 2011;52:2250–2254.
40. Hein K, Gadjanski I, Kretzschmar B, et al. An optical coherence tomography study on degeneration of retinal nerve fiber layer in rats with autoimmune optic neuritis. *Invest Ophthalmol Vis Sci*. 2012;53:157–163.

Investigative Ophthalmology & Visual Science